

Direct shear tests on Mexico City clay with reference to friction pile behaviour

E. OVANDO-SHELLEY

Institute of Engineering, UNAM, Mexico, AP 70-472, Coyoacán, 04510, Mexico City, Mexico

Received 28 January 1994

Accepted 19 November 1994

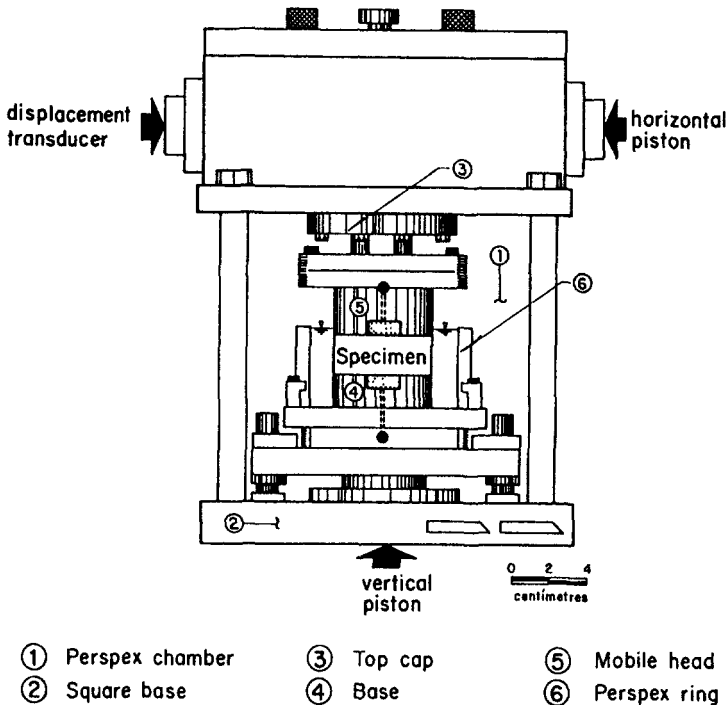
Summary

This paper presents results of static and cyclic direct shear tests performed on undisturbed and remoulded samples of Mexico City clays, including results of 'soil-on-interface' tests. Experiments show that the static adhesion coefficient depends on the soils' liquidity index and that it diminishes due to the effect of repeated dynamic loads. Dynamic overstrength effects were not apparent, as has been observed when testing this clay in other apparatus. Interface strength in remoulded clays is initially less than half the strength of interfaces with undisturbed materials but it increases with time. At least in the materials tested in this research, it did not equal the strength of interfaces with undisturbed materials. Correction factors derived from experimental data can be used to modify the adhesion coefficient to account for dynamic and remoulding effects.

Keywords: Direct shear; interface shear; cyclic; piles; Mexico City clay.

Introduction

Foundation engineering in Mexico City poses extraordinarily complex problems to geotechnical engineers due to the low shear strength and extremely high compressibility of its underlying clay, the effects of regional subsidence and the occurrence of earthquakes. Foundations using friction piles, a common solution in such an environment, have had more problems than any other foundation system during large earthquakes in the past. Inadequate capacity has resulted in large total and differential settlements. However, only a very few buildings founded on friction piles have actually collapsed after or during earthquakes (Rosenblueth and Ovando, 1991). Friction piles have been studied systematically in Mexico City for more than 40 years but there still remain unanswered questions with regard to them. One of these relates to the stress–strain relationships at the pile–soil interface under static and dynamic loads. Large-scale field tests for obtaining these relationships require extensive and reliable instrumentation and are therefore quite expensive. It is not surprising therefore, that very few field tests on well-instrumented friction piles have been reported in the literature. Laboratory testing of soils sheared against other materials can be used as an alternative to gain insights into the characteristics of the stress–



General Set up

Fig. 1a. Direct shear apparatus used in the experiments

displacements relationships, and indirectly into the behaviour of friction piles, without excessive effort and at a moderate cost.

A knowledge of the force–displacement characteristic along a pile’s lateral surface can provide a better understanding of the way in which frictional forces change as a function of stress, time and kinematic conditions. All of these factors ought to be considered in the evaluation of skin friction but in usual practice only the stress state in the vicinity of the pile shaft is accounted for either implicitly (total stress approach) or explicitly (effective stress approach). Time-dependent effects on lateral friction, transient or long term, are either ignored altogether or taken into account using empirical factors or increased factors of safety. The underlying assumption in the practitioners’ analyses in relation to the interface is that it behaves as a rigid-plastic material. Consequently, the deformations or strains at the interface, necessary for mobilizing these frictional forces, are not involved in the calculations. Qualitative judgements about the magnitude and distribution of relative soil–pile displacements can be made on many occasions and on this basis it is possible to assess whether or not frictional forces can fully develop.

The importance of the stress–displacement characteristics at the interface has been recognized in the past (e.g. Smith, 1980). Models in which interface behaviour is simulated by a collection of shear springs and dashpots have been available for a number of years. In some finite element

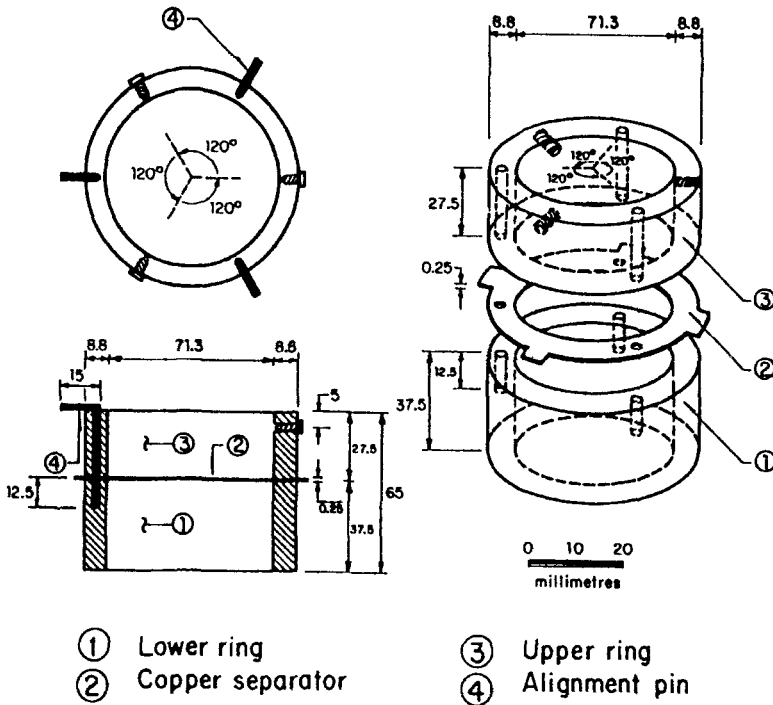


Fig. 1b. Direct Shear rings

programs, frictional elements can also be used to represent soil–pile interfaces and more recently, hybrid finite element–boundary element models have also been proposed (Boulon, 1988). In using these, the stress–strain or force–displacement characteristics at the interface must be specified and yet there are very few experimental data with which to do so.

The experimental results presented herein address some of the questions mentioned previously in connection with the stress–displacement characteristics at the interface under static and dynamic loads, and on the differences in the behaviour between interfaces with undisturbed and remoulded soil. The evolution of strength with time in remoulded materials is also considered.

Experimental techniques

Interface tests have been performed using a variety of devices – direct shear, torsional ring, annular stress and simple shear apparatuses – whose advantages and disadvantages have been discussed previously (Kishida and Uesegui, 1987). A direct shear apparatus was used in this research in which the samples are confined within two rigid rings (diameter = 71.3 mm, total height = 65 mm). Hydraulic actuators apply axial (static) and lateral (static or cyclic) loads which are measured with electronic load cells; a direct current displacement transducer (DCDT) and a dial gauge measure lateral and vertical displacements, respectively. The experimental apparatus is illustrated schematically in Fig. 1a and 1b. Pore pressure measurements were not performed in these tests. Hence, total stresses are used for interpreting the results.

Static vertical stresses were imposed upon the samples to consolidate them. After consolidation, static or cyclic horizontal stresses were then applied. In static tests, shear stresses were applied at a rate of $12.5 \text{ kPa min}^{-1}$; in cyclic tests, samples were sheared with sinusoidal waveforms of varying amplitude and constant frequency (0.5 Hz), which is on average representative of the natural frequency of many soil deposits in Mexico City.

Materials tested

Soils used in this research were retrieved with thin wall samplers from four sites in Mexico City underlain by highly compressible clay strata. Some of the materials were remoulded manually with a spatula for at least 30 min and tested in a disturbed state. Conventional direct shear tests on clay only (soil-on-soil tests, SS tests) and 'soil-on-interface tests' (SI tests) were performed on both undisturbed and remoulded materials.

In the SI tests, clay samples were sheared against a concrete pastille confined by the lower ring in the direct shear apparatus, whilst the upper ring confined the soil (Fig. 1b). The concrete contained volcanic sand and gravel aggregates (maximum size = 12.7 mm, crushing strength $f'_c = 1800 \text{ kPa}$), which are commonly used in the city for making piles. It was saturated to avoid water migrating into it from the soil. The concrete pastilles used in the SI tests had a fairly smooth surface initially and no roughness change was apparent after shearing. Previous work has shown that the shearing resistance between soil and interface depends on the interface's roughness (Potyondy, 1961; Lemos, 1986, etc.). The effect of interface roughness will be addressed in future stages of the experimental programme.

Table 1 indicates the index properties of the materials used in the static loading experiments as well as the type of test performed on each of them.

Tests on undisturbed clay

Static tests

The stress–deformation curves obtained from the tests performed on materials 1, 2 and 4 are given in Fig. 2. Peak strengths mobilized in SI tests were smaller than those obtained from SS tests, with the exception of the tests performed on material 1. The effect of the magnitude of the consolidation pressure was examined in another set of tests performed on material 3 (see Table 1) and is illustrated in Fig. 3. With only three data points the envelopes cannot be established with confidence. However, it would seem that in the SS tests the friction angle at the peak shear stress was 12.8° and in the SI tests, 27.6° but with a smaller cohesion intercept; i.e. the strength at the interface approaches the clay-to-clay strength as the magnitude of the consolidation pressure increases. It may be questionable whether residual conditions were established, as the displacements necessary to attain them in highly plastic clays are rather large. However, from the results shown in Fig. 3, an estimate of the residual friction angle in the SS tests is 21.7° and in the SI tests, 20° .

The results can also be interpreted by means of the ratio between the strength at the interface, C_{ui} , and the strength obtained from the clay-only tests, C_u :

$$\alpha = \frac{C_{ui}}{C_u} \quad (1)$$

Table 1. Conditions for static tests

Material	Test	Sr (%)	Gs	w _f (%)	LL (%)	PL (%)	PI (%)	σ' _v (kPa)	τ _p (kPa)	τ _p /σ' _v
1	SS	100.0	2.47	315.0	338.0	67.0	271.0	57.0	35.0	0.614
	SI	100.0		313.0				57.0	37.9	0.665
2	SS	100.0	2.36	279.0	306.0	108.0	198.0	76.0	100.0	1.31
	SI	97.0		323.0				76.0	87.1	1.14
3	SS	100.0	2.30	263.7	278.0	55.0	223.0	50.0	75.0	1.50
	SS	100.0		255.0				100.0	89.0	0.89
	SS	100.0		270.0				150.0	95.0	0.63
	SI	100.0		299.0				50.0	41.0	0.82
	SI	100.0		293.0				100.0	69.0	0.69
	SI	100.0		288.0				150.0	88.0	0.59
	SI	100.0		288.0				150.0	88.0	0.59
4	SS (0)	100.0	2.50	347.0	322.0	104.0	218.0	66.0	71.3	1.08
	SI (0)	100.0		344.0				66.0	51.8	0.78
	SS ^a (0)	98.0		351.0				66.0	33.2	0.50
	SI ^a (0)	99.0		343.0				66.0	21.7	0.33
	SI ^a (6)	100.0		358.0				66.0	29.9	0.45
	SI ^a (100)	98.0		336.0				66.0	46.6	0.71
	SI ^a (100)	98.0		336.0				66.0	46.6	0.71

w_f = water content after consolidation; σ'_v = vertical effective stress during consolidation; τ_p = maximum shear stress; SS = soil on soil test; SI = soil on interface test.

^a Tests on remoulded soil (numbers in brackets indicate hours after primary consolidation, before failure stage).

Clearly, α is analogous to the adhesion coefficient used in the total stress approach for evaluating lateral friction in piles. The experimental results can be conveniently represented by plotting the values of α against liquidity index (LI).

Figure 4 shows the dependence of α on LI. Despite the limited number of tests, a general trend can be seen. For very wet materials (LI > 1) α is less than unity, but appears to tend towards unity as LI decreases. Values of the adhesion coefficient for piles driven into soft Mexico City clays are generally taken to be close to 1.0, which in general agrees with the experimental data presented here, whereas α values for lower plasticity clays are normally quoted as being less than unity.

Cyclic tests

SS and SI tests were performed on materials 1 and 2, applying cyclic shear stresses until failure of the specimen was achieved. Testing conditions are summarized in Table 2. In some cases the tests were interrupted when failure was not brought about after a few thousand cycles. The graph in Fig. 5 shows dynamic stress–deformation curves for a soil-on-soil test on material 1 with a cyclic shear stress of 28.9 kPa which is typical of the behaviour observed.

In these experiments, material 1 was stronger in the SI tests than in the SS tests and material 2 the opposite. This tendency is similar to that observed in the static tests. The number of cycles to reach failure for the range of cyclic stress amplitudes, expressed as a fraction of the static

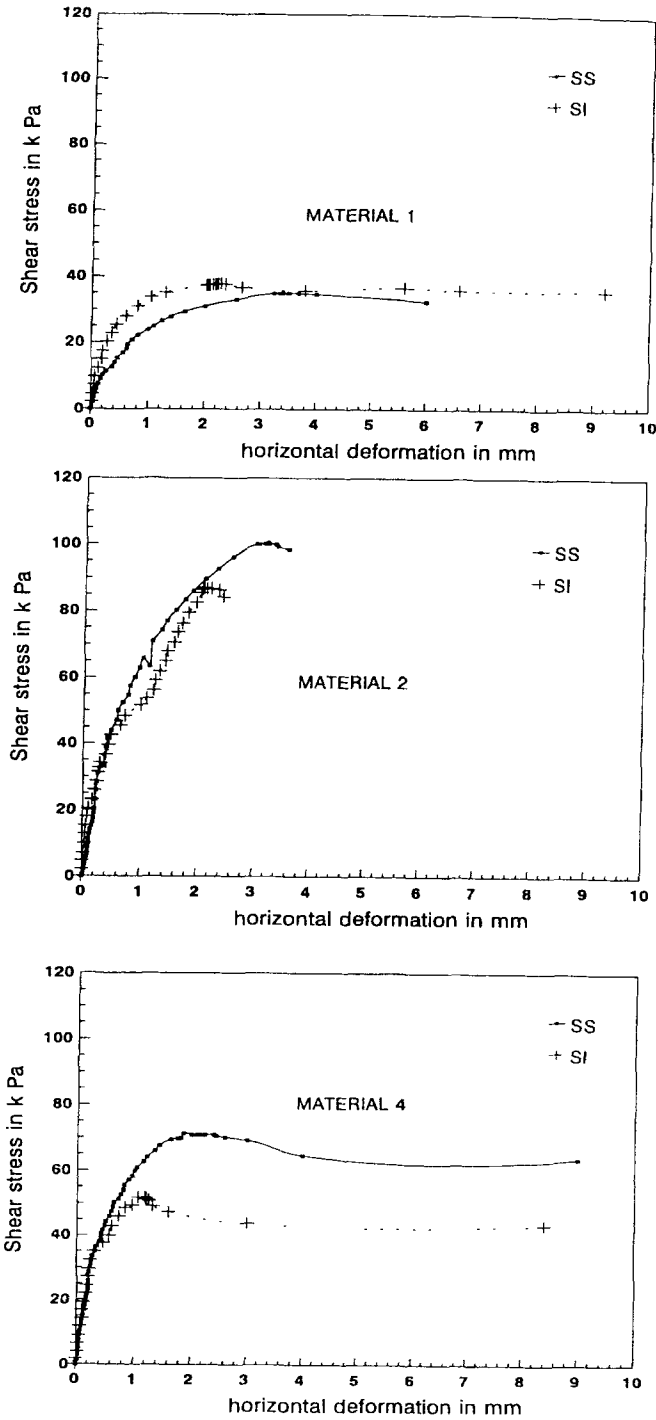


Fig. 2. Stress–deformation curves from static soil-on-soil (ss) and soil-on-interface (SI) tests

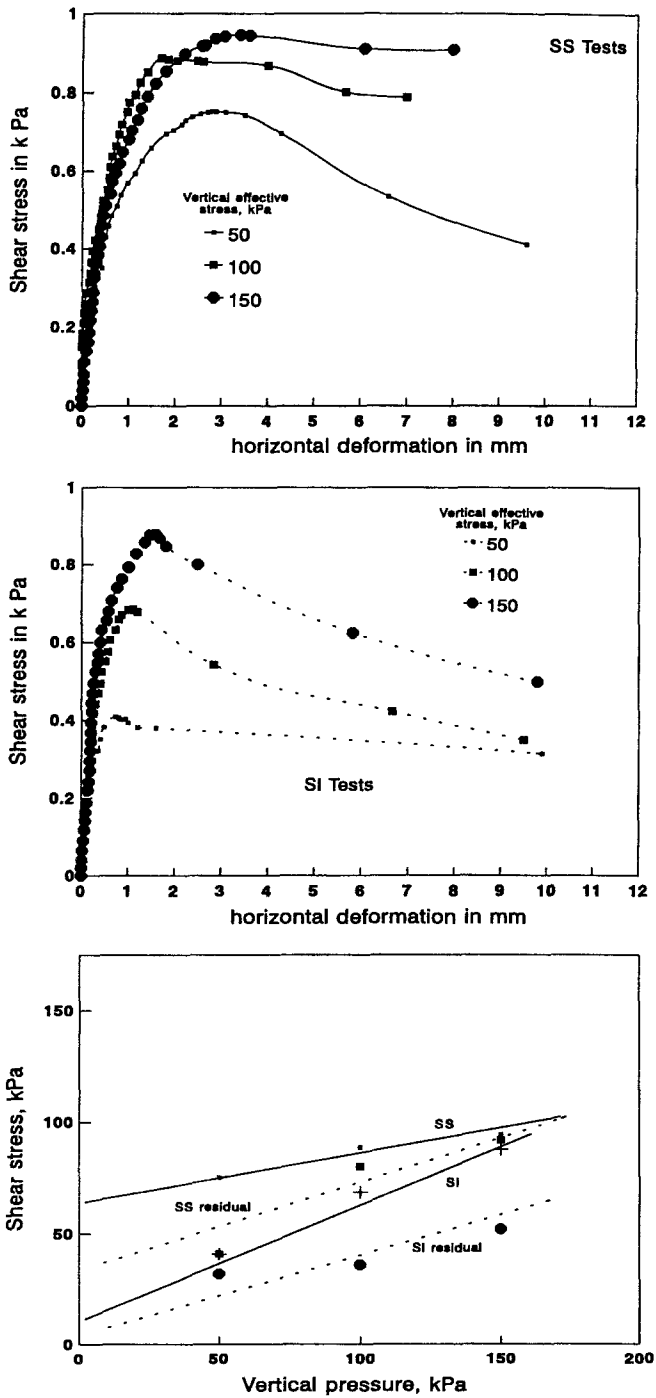


Fig. 3. Peak and residual strength envelopes from static direct shear tests

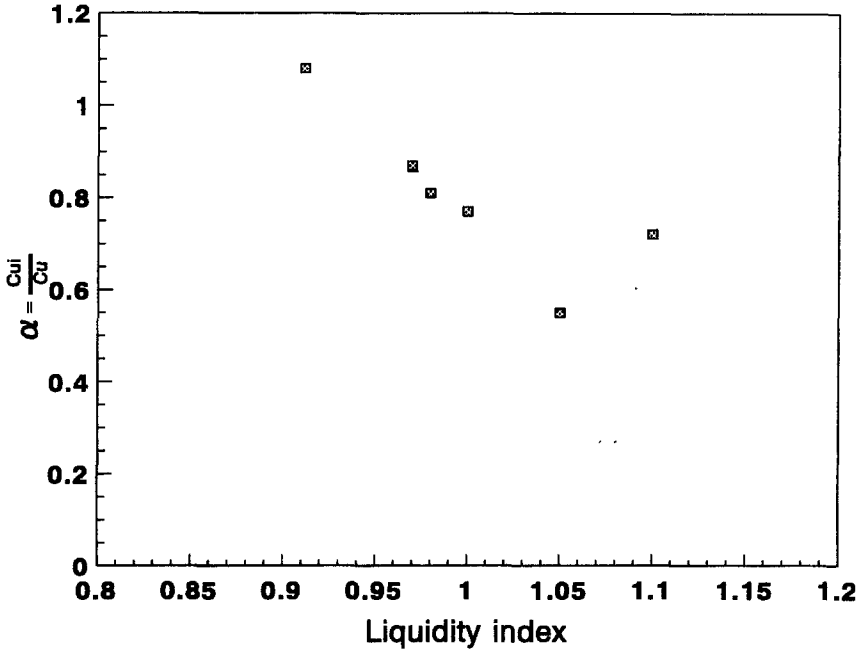


Fig. 4. Experimental relationship between the adhesion coefficient and liquidity index

Table 2. Conditions for cyclic tests

Material	Tests	Sr (%)	Gs	w _f (%)	LL (%)	PL (%)	α'_v (kPa)	τ_{cyc} (kPa)	τ_{cyc}/τ_{st}	N _f
1	SS	100.0	2.47	329.0	338.0	67.0	57.0	23.6	0.67	126
	SS	100.0		306.0				28.9	0.82	7
	SS	100.0		303.0				34.1	0.97	<1
	SI	99.0		327.0				25.3	0.67	1000 ^a
	SI	100.0		313.0				35.4	0.93	141
	SI	98.0		306.0				36.8	0.97	<1
2	SS	100.0	2.36	268.0	306.0	108.0	76.0	49.3	0.49	6000 ^a
	SS	96.0		202.0				69.7	0.70	115
	SS	100.0		280.0				98.0	0.98	3
	SI	99.0		213.0				41.7	0.48	821
	SI	100.0		257.0				59.5	0.68	<1
	SI	97.0		223.0				62.5	0.72	<1

τ_{cyc} = cyclic stress amplitude; τ_{st} = static shear stress at failure; N_f = number of cycles applied to the samples.

^a Samples in which failure was not reached.

strength, τ_{cyc}/τ_{st} , is shown in Fig. 6. The data given in Table 2 show that for all the tests, $\tau_{cyc}/\tau_{st} \leq 1$; i.e. it was never possible to perform tests in which the cyclic stress amplitude exceeded the static strength ($\tau_{cyc}/\tau_{st} > 1$) as samples in which that condition was attempted failed during the first cycle. This implies that dynamic overstrength effects do not develop in

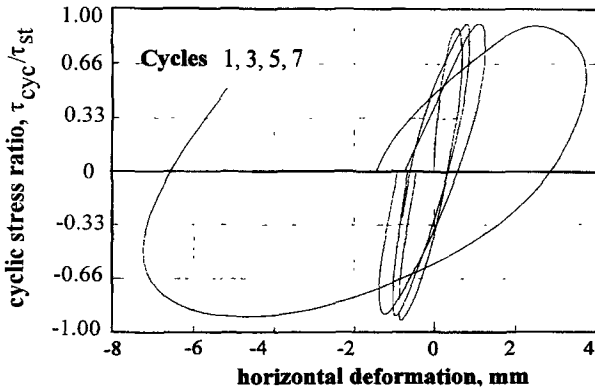


Fig. 5. Typical cyclic stress–deformation curve (material 1, soil-on-soil test)

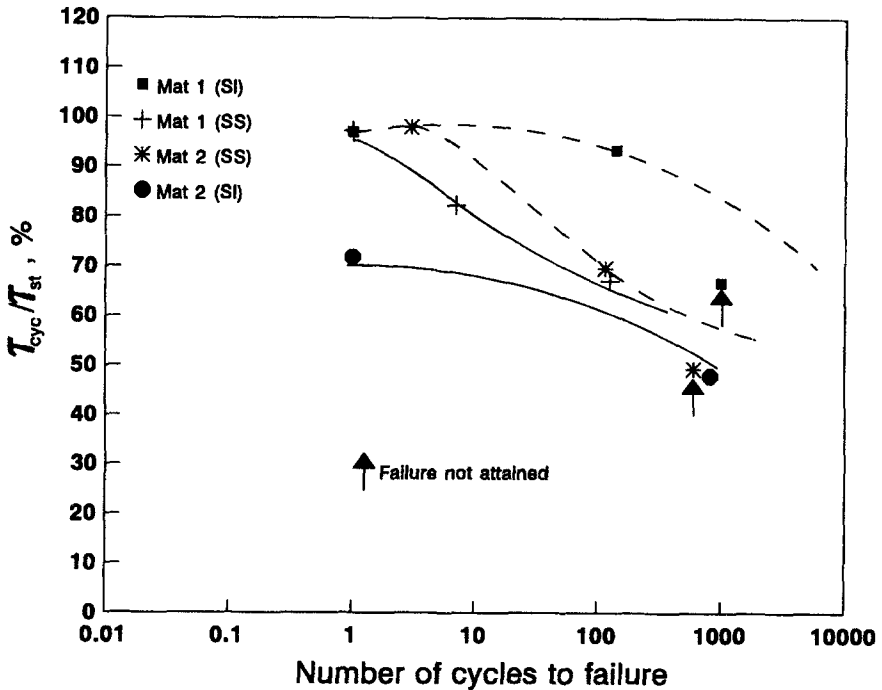


Fig. 6. Relationship between the number of cycles to failure and the cyclic stress amplitude

these tests as opposed to what has been observed previously when testing Mexico City clays in either cyclic triaxial cells (Romo, 1990), the simple shear apparatus (Cuanalo, 1993) or a hollow cylinder apparatus (M.J. Mendoza, personal communication, 1993). The cyclic stress ratio necessary to produce failures at a moderate number of cycles (say, less than 100) is at least 0.6.

Deformations during cyclic loading accumulate at a nearly constant rate with the logarithm of the number of applied cycles until the critical number of cycles (N_{crit}) is reached; thereafter, they accumulate at increasingly higher rates and failure follows shortly after N_{crit} (Fig. 7). This feature

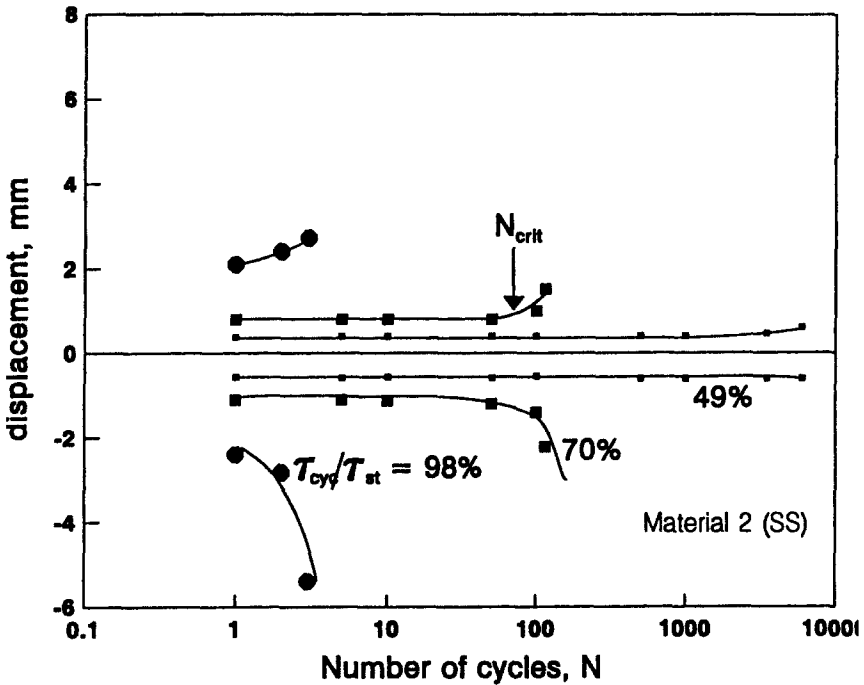


Fig. 7. Evolution of shear displacements in terms of the number of applied load cycles for different stress amplitudes

has been observed repeatedly in previous dynamic tests on many other soils. The relationship between τ_{cyc}/τ_{st} and N_{crit} is given in Fig. 8. Figures 7 and 8 reflect the fact that strength and stiffness degrade as cycling of shear stresses is in progress. The ordinate of Fig. 8 can be interpreted as a reduction factor for the shear strength due to the effects of cyclic loads, i.e. as a fatigue factor. For the seismological and geotechnical conditions that prevail in Mexico City, fatigue effects may be far from negligible during large earthquakes in which nearly monochromatic wave trains of fairly constant amplitude have been recorded. Seismic axial overloading on piles due to moments that act upon buildings during an earthquake would also be nearly monochromatic. A fatigue factor, β , can be used to reduce the frictional capacity of piles for any given value of N or N_{crit} . If excessive relative deformations at the soil–pile interface are to be avoided, β should be taken as the τ_{cyc}/τ_{st} value for the appropriate value of N_{crit} . The reduced frictional capacity at the interface can therefore be expressed as

$$C_{ui} = \alpha\beta C_u \tag{2}$$

For practical application of the fatigue curves, earthquakes loading must be converted into an equivalent sinusoidal wave of constant amplitude and frequency by means of the concept of the equivalent number of cycles (e.g. Lee and Chan, 1972).

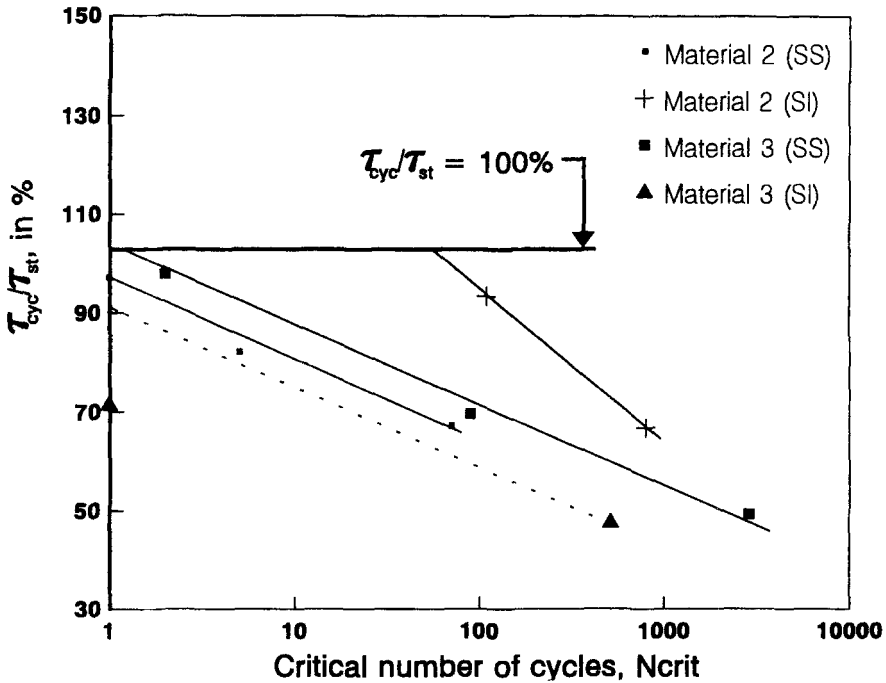


Fig. 8. Relationship between the critical number of cycles and the normalized stress amplitude

Tests on remoulded clay

In these tests, samples were formed by remoulding material 4, as explained previously, at the same water content as the soils in their undisturbed state (35% on average). The soil was then moulded into the confining rings in the direct shear apparatus and consolidated under a vertical stress approximately equal to the *in situ* effective horizontal stress of the original undisturbed material (66.0 kPa). The consolidation stress was applied in small, fast increments (50 kPa min⁻¹). Shear stresses were then applied after 0.0, 6.0 and 100.0 h after the end of primary consolidation. Testing conditions are summarized in Table 1. The resulting stress-displacement curves are given in Fig. 9.

Experimental results show that remoulded specimens sheared immediately after primary consolidation lose 47 and 42% of their undisturbed strengths in SS and SI tests, respectively. Samples that were allowed to consolidate after the end of primary consolidation gain strength as the consolidation time increases. The results can be interpreted in terms of three strength ratios:

$$\alpha_1 = \frac{C_{wir}}{C_{ur}}; \quad \alpha_2 = \frac{C_{uir}}{C_{ui}}; \quad \alpha_3 = \frac{C_{uir}}{C_{ur}} \tag{3}$$

where C_{wir} = remoulded undrained strength at the interface; C_u = undrained strength of the undisturbed clay alone; C_{ui} = undrained strength of the undisturbed clay sheared on an interface; C_{ur} = undrained strength of the remoulded clay alone.

The variation of the strength ratios with time is shown in Fig. 10; in it the abscissae were normalized with respect to the time for 100% primary consolidation. The three ratios tend asymptotically to constant values. The lower curve (α_1) indicates that the remoulded strength at

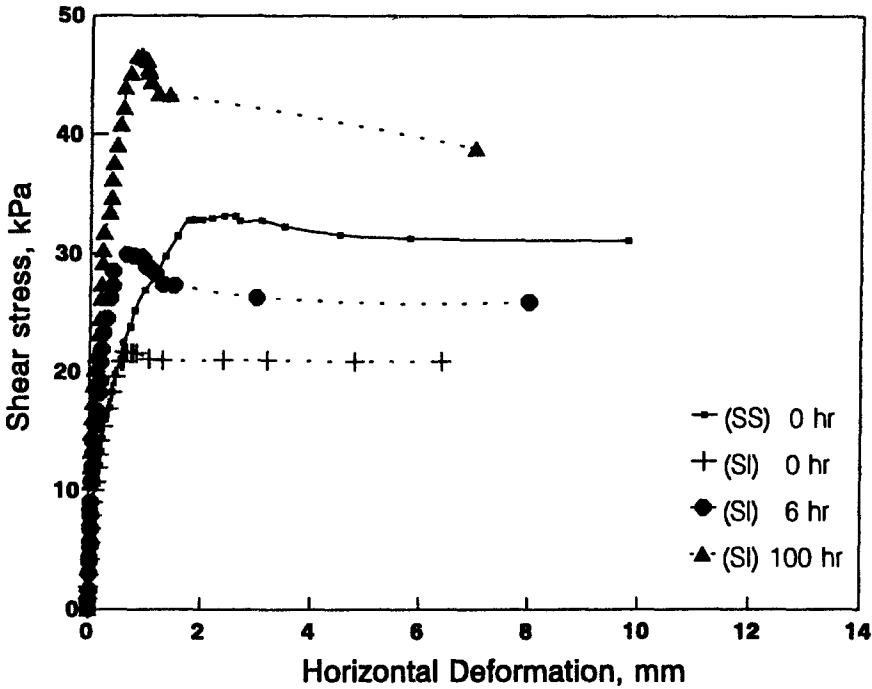


Fig. 9. Results of static direct shear tests on remoulded clays with different consolidation times

the interface will only be slightly higher than half the intact material’s strength; α_1 is the adhesion coefficient for the remoulded materials.

From equations 1 and 3:

$$\frac{C_{uir}}{C_{ui}} = \frac{\alpha_1}{\alpha} = \alpha_2 \tag{4}$$

i.e. α_2 is a correction factor for the adhesion coefficient that accounts for remoulding effects. This tends to a value of about 0.7 for long-term conditions (Fig. 10). Finally, the upper curve in Fig. 10 indicates that the remoulded strength at the interface can be about 40% higher than the initial remoulded strength measured in a conventional direct shear test. It should be obvious that the shape of the curves in Fig. 10 will vary from soil to soil. In less thixotropic materials, strength gains after primary consolidation ought not to be as important.

The curves in Fig. 10 can be modelled approximately by means of hyperbolas of the form

$$\alpha_i(T^*) = \frac{T^*}{a_i + b_i T^*} + \alpha_i(0) \quad i = 1, 2, 3 \tag{5}$$

where a_i and b_i are experimental parameters and $\alpha_i(0)$ are the initial values of α_i . The values of $\alpha_i(0)$, a_i , and b_i determined from the experimental data are given in Table 3.

If, for the sake of simplicity, Terzaghi’s assumptions for one-dimensional consolidation are assumed to hold along horizontal planes perpendicular to the pile axis, the time ratio T^* can be expressed as:

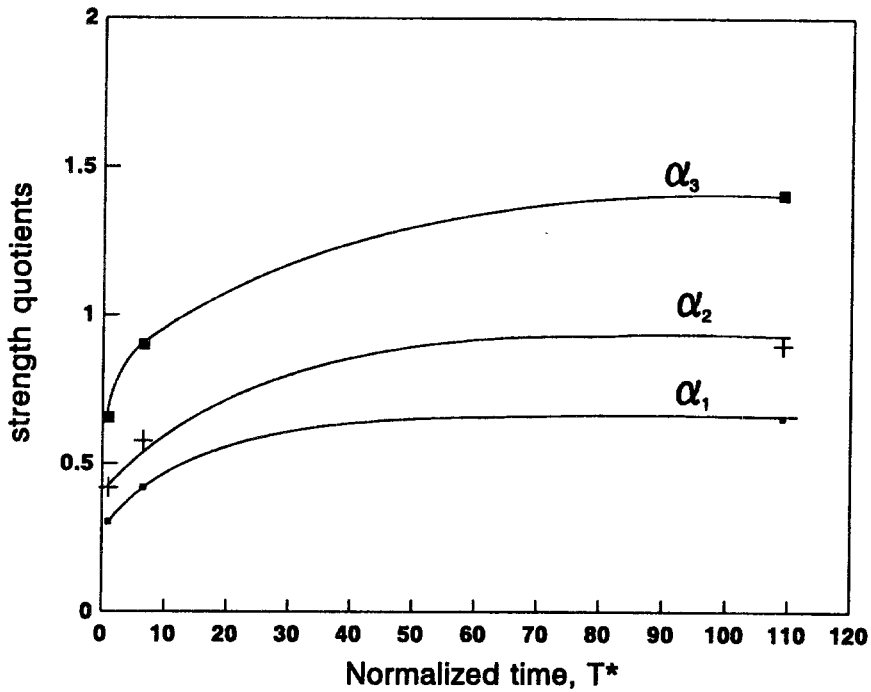


Fig. 10. Evolution of the strength quotients with normalized time

Table 3. Coefficients of equations relating α to T^* determined from the experiments

i	$\alpha_i(0)$	a_i	b_i
1	0.28	39.49	2.33
2	0.30	28.71	1.70
3	0.61	18.29	1.10

$$T^* = \frac{t}{t_{100}} = c_{vr} \frac{t}{R^2} \tag{6}$$

where c_{vr} is the consolidation coefficient of the remoulded soil and R the length of the drainage path. If Equation 5 is to be applied to piles, it must be modified to account for the actual boundary conditions in the remoulded soil along a pile. The one-dimensional assumption for consolidation can be used as an approximation assuming R to be the width of the remoulded zone, or half that length, in the case of concrete piles, assuming that water will flow from the remoulded zone into the surrounding soil and into the pile itself. R can be obtained from the theory of cavities or expanding cavities in elasto-plastic media as a function of Cu and the soil's stiffness (undrained Young's modulus or shear modulus). A hypothesis is also required with regard to the initial pore pressure distribution; cavity expansion theory, for example, predicts that initially pore pressure varies with the logarithm of R , with a maximum at the pile face and zero excess pore pressure at R (Leifer *et al.*, 1980).

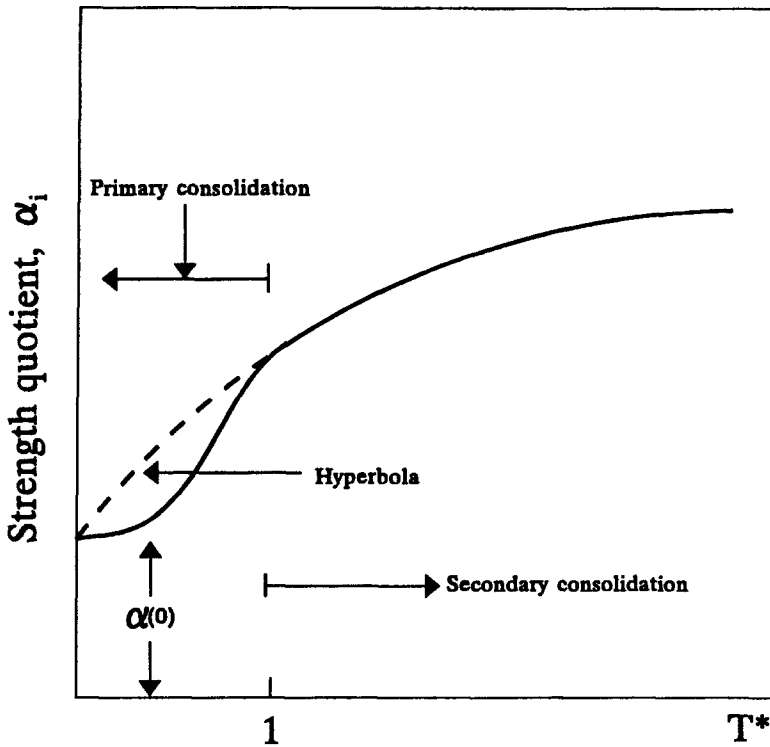


Fig. 11. Schematic representation of Equations 7 and 8

Under Terzaghi's assumptions Equation 5 is no longer hyperbolic for $T^* < 1$ and is given by

$$\alpha_i(T^*) = \frac{F(T_v)}{a_i + b_i} + \alpha_i(0)[1 - F(T_v)] \tag{7}$$

where $F(T_v)$ is the one-dimensional consolidation function for the appropriate initial and boundary conditions. Equation 7 implies that the gain in strength is proportional to the increase of effective stresses during primary consolidation. For $T^* > 1$ the resulting expression is

$$\alpha_i(T^*) = \frac{1}{a_i + b_i} + \frac{T^*}{a_i + b_i T^*} \tag{8}$$

The values of $\alpha_1(0)$ and $\alpha_2(0)$ provide an approximate measure of the remoulding action causing the destruction of the structure of the initially undisturbed clay. Comparing these values with those obtained with Equation 7 for $T > 0$, the relative influence of primary consolidation can also be assessed. With the use of Equation 8, the effect of secondary consolidation can also be accounted for. In the case of the materials tested in this research, the latter is the most important factor. Equations 5, 7 and 8 are plotted schematically in Fig. 11.

How these expressions could be applied in a practical situation is provided by the following example: in a 30 cm diameter concrete pile driven into Mexico City clay ($G/Cu = 37$, $C_{vr} = 0.001 \text{ cm}^2 \text{ s}^{-1}$) the plastic zone around its shaft would be about six times its radius according to cavity expansion theory. The plastic zone would take at least 17 days to consolidate

assuming that the initial excess pore pressure is uniformly distributed within the remoulded zone. Long-term conditions, say for $T^* = 100$, would ensue after nearly five years.

Finally, introducing dynamic fatigue and remoulding effects, the strength at the interface expressed in terms of the strength of the undisturbed material is:

$$C_{uir} = \alpha \cdot \alpha_2(T^*) \cdot \beta(\tau/\tau_f, N) \cdot C_u \quad (9)$$

Discussion and conclusions

From direct shear soil-on-soil and soil-on-interface tests, a relationship has been established between the adhesion coefficient and liquidity index. This coefficient tends to one as LI decreases and the consolidation pressure increases; i.e. as the strength at the concrete–clay interface tends towards the strength of the clay alone.

The dynamic tests showed that the strength and stiffness of Mexico City clay in the direct shear apparatus degrade considerably due to the effects of repeated loading. Experiments also show that dynamic overstrength is absent when this material is tested in the direct shear apparatus. A fatigue factor, expressed in terms of the ratio between cyclic shear stress amplitude and static strength, was obtained from the results of these tests. The fatigue factor depends, for a given cyclic shear stress amplitude, on the number of stress reversals and it turns out to be, at most, equal to unity.

Static soil-on-interface tests using remoulded materials yield strengths as low as 42% of the strength obtained from the same test performed on undisturbed material. The experiments also show that for time ratio $T^* < 1.0$ strength increases are proportional to changes in effective stresses and as a first approximation to evaluate this, one-dimensional consolidation theory can be used. For $T^* > 1.0$, strength tends asymptotically towards a constant value. On the basis of these results, a time-dependent reduction factor for the adhesion coefficient has also been derived which, for the long-term condition is equal to about 0.7. It is very likely that strength gains after consolidation will be less important in other less thixotropic clays.

The fatigue and the remoulding factors can reduce considerably the available strength at the interface. In actual piling applications, these reductions would be compensated for, at least partially, by the increase of lateral stresses brought about by pile-driving. The magnitude of these stress changes will depend on the geometry of the pile section and on the size of preboring, relative to the pile section. In the case of driven piles without preboring, mean effective stresses in the vicinity of the pile would theoretically be between 1.5 and 3.7 times larger than the *in situ* stress, depending on the relative stiffness of the intact and the remoulded soil (Leifer *et al.*, 1980). For preboring sizes equal to the actual pile diameter, stress changes would depend on other factors such as the use or not of stabilizing fluids. In the former, the results of the soil-on-soil tests would be applicable since failure would occur within the clay, some distance from the pile face whereas in the latter case, in which failure is likely to develop at the pile–clay interface, the soil-on-interface test results would be more relevant.

Acknowledgements

The tests described in this paper were performed by Oscar Cuanalo with the aid of Gonzalo Roque, using the experimental facilities of the research lab at the Department of Soil Mechanics

of the Graduate School of Engineering, UNAM, Mexico City. Their help is duly acknowledged and the suggestions and comments of Dr M.P. Romo are greatly appreciated.

References

- Boulon, M. (1988) *Contribution a la mecanique des interfaces sol-structures*, Memoire d'habilitation, Joseph Fourier University, Grenoble.
- Cuanalo, O. (1993) Estudio experimental de interfaces arcilla-concreto (Experimental study of clay-concrete interfaces), MSc Thesis, Graduate School of Engineering, UNAM, Mexico.
- Kishida, H. and Uesegui, H. (1987) Tests of the interface between sand and steel in simple shear apparatus, *Géotechnique*, **37**, 1, 45–52.
- Lee, K.L. and Chan, K. (1972) Number of equivalent significant cycles in strong motion earthquakes, in *Proceedings of the International Conference on Microzonation*, Seattle, Washington, 1972, Vol. 11, pp. 609–17.
- Leifer, S.A., Kirby, R.C. and Esrig, M.I. (1980) Effect of radial variation in modulus on stress after consolidation around a driven pile, in *Proceedings of the Conference on Numerical Methods in Offshore Piling*, London, 1979, The Institution of Civil Engineers, pp. 157–63.
- Lemos, L. (1986) The effect of rate of shear on the residual strength of soil, PhD Thesis, Imperial College, University of London.
- Potyondy, J.G. (1961) Skin friction between various soils and construction materials, *Géotechnique*, **11**, 339–53.
- Romo, M.P. (1990) Comportamiento dinámico de la arcilla de la ciudad de México y su repercusión en la ingeniería de cimentaciones (Dynamic behaviour of Mexico City Clay and its impact on foundation engineering), in *Proceedings of the Symposium on The Subsoil of Mexico City and its Relationship with Foundation Engineering*, Mexico City, 1991, The Mexican Society for Soil Mechanics, pp. 83–94.
- Rosenbleuth, E. and Ovando, E. (1991) Geotechnical lessons learned from Mexico and other recent earthquakes, in *Proceedings of the Second International Conference on Recent Advances on Geotechnical Earthquake Engineering and Soil Dynamics*, St Louis, Missouri, 1991, University of Missouri, Rolla, Vol. 2, pp. 1799–819.
- Smith, I. M. (1980) A survey of numerical methods in offshore piling, in *Proceedings of the Conference on Numerical Methods in Offshore Piling*, London, 1979, The Institution of Civil Engineers, pp. 1–8.